

Nonlinear dynamics induced by burst amplification in optically gain-stabilized erbium-doped amplifiers

G. Della Valle, A. Festa, and S. Taccheo

Politecnico di Milano—Dipartimento di Fisica, Piazza Leonardo da Vinci 32, 20133 Milan, Italy

K. Ennser

University of Wales Swansea—Institute of Advanced Telecommunications, Swansea, UK

J. Aracil

Universidad Autonoma de Madrid, Ciudad Universitaria de Cantoblanco, 28049 Madrid, Spain

Received January 2, 2007; accepted January 9, 2007;

posted January 23, 2007 (Doc. ID 78393); published March 19, 2007

Optical burst amplification in a gain-stabilized amplifier may generate complex gain dynamics with nonlinear behavior. This phenomenon is thoroughly investigated by using a theoretical model and dedicated experiments. Design guidelines for optimized devices avoiding optical burst transmission impairments are proposed. © 2007 Optical Society of America
OCIS codes: 060.2320, 060.2330, 060.2410.

Optical burst transmission is a very promising way to implement Internet Protocol traffic by WDM and to guarantee payload transparency as well as a more efficient bandwidth utilization with respect to other solutions.¹ However, to properly amplify optical bursts, the optical amplifier (OA) should be stabilized to avoid burst distortions due to total input power variations. Electronic and optical gain control techniques have been proposed,^{2,3} but extreme conditions, such as the simultaneous drop of all but one WDM burst channels, may cause unacceptable amplitude variations of the surviving channel. Recently, by using a proper design of an optical gain-clamped (OGC) waveguide amplifier, we demonstrated immunity to transients due to add-drop operation or network restoring.⁴ More recently we tested the same device in optical burst transmission and noticed a complex behavior when the repetition rate of the bursts approaches the natural device relaxation oscillation frequencies,⁵ with some analogy to extremely low-gain lasers.⁶ The use of the OGC optical amplifier (OGC-OA) for optical burst transmission was therefore questionable, and a deeper investigation is necessary to evaluate possible deleterious transmission impairments.

In this Letter we report the results obtained by an extensive investigation of these phenomena. In particular, we evaluate the effect of input power, pump power level, and cavity length on burst transients. The abrupt resonances and nonlinear behavior reported in Ref. 6 are confirmed, and we also show that a burst sequence may generate very complex dynamics with different periodicity. Supported by experiments and a suitable numerical model, we show that the impairments may be strongly reduced by decreasing the cavity length.

To investigate this issue we use a 30 cm long highly doped silica fiber and the OGC erbium-doped fiber

amplifier (OGC-EDFA) setup shown in Fig. 1(a). The laser cavity is formed by two fiber Bragg gratings (FBGs) with a 1550 nm center wavelength and reflectivities of 99.8% (HR FBG) and 95%. The signal channels are injected into the EDFA through a 90%/10% splitter. The variable optical attenuator (VOA) allows gain tuning.⁷ In our experiment the cavity length is set to 12 m, thus comparable with a standard EDFA (a few tens of meters), and we have evaluated the transient induced on a single channel in the worst case of all the other 15 burst channels arriving or dropping at the same time. We represent 15 burst channels' input power by introducing one signal with -1 dBm peak power into the OGC-OA at wavelength $\lambda_{\text{mod}} = 1537$ nm. The light at 1537 nm is modulated by an acousto-optic modulator with a variable repetition rate and a duty cycle of 50%. To analyze the OA gain dynamics, we use a -13 dBm probe signal, representing the surviving channel out of 16 channels, provided by a continuous wave distributed feedback laser at $\lambda_{\text{probe}} = 1553$ nm. Modulated channels and the probe channel are combined by means of a 50% coupler before entering the amplifier. With -1 dBm input power the pump power level for clamping (i.e., laser) threshold is 170 mW, and operating 14% above laser threshold (namely, at 194 mW of pump power),

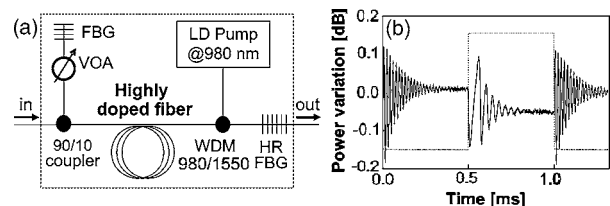


Fig. 1. (a) Experimental setup of the OGC amplifier. (b) Probe channel output variation at 1 kHz burst repetition rate. Burst peak power is -1 dBm. Dotted line, ON-OFF time slots.

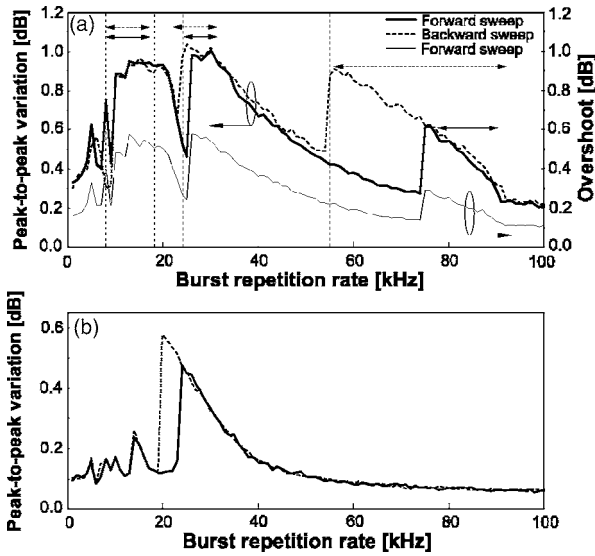


Fig. 2. (a) Peak-to-peak variation versus burst repetition rate for the worst case of 15 out of 16 bursting channels. Bottom curve, forward sweep overshoot only. Horizontal arrows indicate $2T$ waveform intervals (solid arrows, forward sweep; dashed arrows, backward sweep). Vertical lines define $\nu_{\text{add}}/3$, $\nu_{\text{drop}}/3$, ν_{add} , ν_{drop} . (b) Peak-to-peak variation versus burst repetition rate for power modulation of 1/4 with respect to case (a).

the OGC-OA provides an almost flat 14 dB gain in OGC mode over the whole C band.

Figure 1(b) shows the variations in the output power of the probe channel when the saturating channels (15 burst channels) are ON-OFF modulated at 1 kHz. The variation is dumped within each time slot toward the steady-state condition, and a maximum peak-to-peak variation of about 0.3 dB is measured. We use as reference the output power level with single-channel input. The steady-state power level decrease with full channel load is due to a spectral hole-burning (SHB) effect.⁷ Figure 1(b) clearly shows that our OGC-OA has two characteristic relaxation oscillation frequencies: $\nu_{\text{drop}} \approx 55$ kHz after a drop operation (no burst channels) and $\nu_{\text{add}} \approx 24.2$ kHz after an add (all burst channels on).

Figure 2(a) shows the measured peak-to-peak gain variation of the amplifier with respect to burst repetition rate ν . The solid upper curve shows the result when we sweep the repetition rate from 0 to 100 kHz, and the dashed curve shows the result during the backward sweep. We note the presence of sharp resonances and a strong hysteretic behavior. A 1 dB gain maximum excursion in a quite large frequency range is measured. The floor value at the low repetition rate is due mainly to SHB. Note that the transient value is equally due to overshoot and undershoot, as can be seen in Fig. 2(a), where the bottom curve shows the overshoot variation only.

We further investigated the transient at different frequencies and noticed a bistable behavior in resonance frequency ranges indicated by horizontal arrows in Fig. 2(a), with a periodicity that is usually double ($2T$) the burst repetition period ($T=1/\nu$). As an example, Fig. 3 shows some of the most interesting waveforms recorded: at 10 kHz, which is on the

very left edge of the first resonance of Fig. 2(a), we observe bistable behavior of the system between a waveform of period T (Fig. 3, black curve) and a waveform of period $2T$ (Fig. 3, gray curve). Top traces in Fig. 3 show that at a 19 kHz repetition rate, well within resonance, bistable behavior is between two waveforms of the same periodicity $2T$. In Fig. 2(b) we also show the experimental results with significantly lower input power modulation (total input power of -4 dBm and 50% drop). As can be seen, the gain variation is strongly reduced, to approximately one-half in the decibel scale, and the resonance at around 80 kHz disappears.

The above experiments demonstrate that a standard OGC-EDFA may suffer transmission impairments. However, by means of a proper design of the amplifier, and considering the statistical behavior of real burst traffic, an OGC-OA that is almost insensitive to burst transients even in the worst case can be demonstrated. To pursue this goal, we developed a suitable simplified model of our device by applying the stability analysis to the OGC-OA configuration reported in a previous paper.⁸ In our model the optical clamped amplifier is seen as a perturbed laser system, where signal powers act as a negative pump. With n_2 being the population of the upper laser level averaged along the length of the active medium, and P_L the intracavity power at the lasing wavelength, the space-independent rate equations system describing the laser is

$$\frac{dn_2}{dt} = -\frac{n_2}{\tau_{21}} + R_P^{\text{eff}} - K_{\text{up}}n_2^2, \quad (1)$$

$$\frac{dP_L}{dt} = \frac{G^2\Gamma^2 - 1}{2(L_e/c)}P_L, \quad (2)$$

where K_{up} is the upconversion constant, G and Γ are single-pass gain and loss, respectively, and L_e is the optical length of the cavity. R_P^{eff} is the effective pump rate, accounting for the actual pump rate R_P , the amplified N channels, and the intracavity laser power, which decrease erbium inversion (thus acting as a negative pump):

$$R_P^{\text{eff}} = R_P - \sum_{i=1}^N \frac{P_{\text{in}}^i}{h\nu_s A_b l} (G - 1) - \frac{P_L}{h\nu_L A_b l} (G^2 - 1), \quad (3)$$

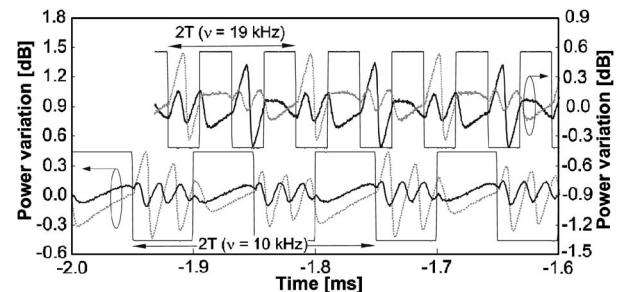


Fig. 3. Waveforms recorded at 10 kHz (bottom) and 19 kHz (top); backward sweep. We show that in both cases two waveforms may occur.

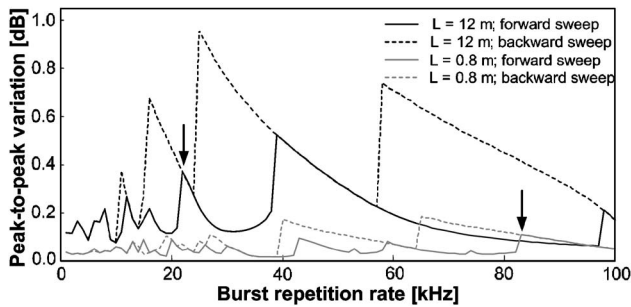


Fig. 4. Effect of cavity length reduction on transient overshoots. Upper traces, $L=12$ m; lower traces, $L=0.8$ m. Arrows indicate corresponding peaks at $\nu_{\text{drop}}/3$.

where the output power of the i th channel is $P_{\text{out}}^i = GP_{\text{in}}^i$. We considered a two-channel system and numerically integrated Eqs. (1) and (2) by a Runge-Kutta method with proper initial conditions. Note that both amplified spontaneous emission and SHB effects are disregarded. Despite such approximations, our model results are sufficiently accurate to predict all the particular features of the OGC-EDFA observed, such as hysteresis, abrupt and asymmetric resonances, and double-period waveforms in the surviving channel gain dynamics. As a significant result we show in Fig. 4 the theoretical prediction in the case of an overthreshold of $x=1.6$ with two cavity lengths, namely $L_1=12$ m and $L_2=0.8$ m. Note that, as expected, the increase in overthreshold (with respect to the value of $x=1.14$ used in the experiments) reduces peak-to-peak variations, but the shortening of the cavity length results in a more effective and cost-free solution. In fact, the peaks are strongly reduced by a factor of $(L_1/L_2)^{1/2} \approx 4$ (see arrows in Fig. 4) as expected from OGC-OA theory. The latter solution also shifts dangerous resonance frequencies to higher values, potentially above 100 kHz, which can be assumed to be the upper limit of the burst transmission frequency range.

Note that the above investigation refers to the worst case of infinitely long burst sequences, but in real traffic the sequences are finite. Therefore we also evaluated the probability of having a burst sequence of a given length. Burst sequences can actually happen with a time-based burstifier,⁹ which we applied for our case assuming that burst sequences arrive following a Poisson process. As an example, we estimated that the probability of having sequences of more than two bursts at $\nu=40$ kHz [which is within

one of the strongest resonances in Fig. 2(a)] is below 1%. Moreover, in the case of a two-burst sequence at $\nu=40$ kHz, the simulation predicts a peak-to-peak gain variation of only 0.2 dB instead of the value of about 0.6 dB reported in Fig. 2(a). Therefore the induced impairment in real burst traffic is expected to be lower than the one reported above.

In conclusion, we have investigated in depth the dynamic behavior of optically gain-clamped amplifiers for optical burst transmission. We have demonstrated that a careful design using a compact gain medium results in very limited induced transients with peak resonance frequencies out of burst transmission frequency range. Therefore, also considering that the probability of long burst sequences is low in real burst traffic, an OGC-OA immune to burst gain impairments can be realized.

Authors acknowledge partial support by Ministero dell'Università e della Ricerca Italy project 2005099872, by Network of Excellence e-Photon/One+ JP-B, and by COST action 291. S. Taccheo's e-mail address is taccheo@polimi.it.

References

1. Yu-Li Hsueh, J. Kim, Ching-Fong Su, R. Rabbat, T. Hamada, C. Tian, and L. G. Kazovsky, *J. Lightwave Technol.* **24**, 44 (2006).
2. A. Lieu, C. Tian, and T. Naito, in *Optical Fiber Communication Conference and Exposition and the National Fiber Optic Engineers Conference*, Technical Digest (CD) (Optical Society of America, 2005), paper OtuD5.
3. M. Zirngibl, *Electron. Lett.* **27**, 560 (1991).
4. T. Rogowski, S. Taccheo, J. Shmulovich, and K. Ennser, in *31st European Conference on Optical Communications 4*, (Institution of Electrical Engineers, 2005), pp. 919–920.
5. G. Della Valle, A. Festa, S. Taccheo, and K. Ennser, in *32nd European Conference on Optical Communications* (Société de l'Electricité, de l'Electronique et des Technologies de l'Information et de la Communication, 2006), paper We3.P.29.
6. L. Luo, T. J. Tee, and P. L. Chu, *J. Opt. Soc. Am. B* **15**, 972 (1998).
7. K. Ennser, T. Rogowski, J. Shmulovich, and S. Taccheo, *Opt. Express* **14**, 10307 (2006).
8. K. Ennser, G. Della Valle, M. Ibsen, J. Shmulovich, and S. Taccheo, *IEEE Photon. Technol. Lett.* **17**, 1468 (2005).
9. X. Yu, J. Li, Y. Chen, and C. Qiao, *J. Lightwave Technol.* **22**, 2722 (2004).